

13.6 A conceptual dual-polarization framework for the 8 May 2003 Oklahoma City tornadic supercell

Glen S. Romine*

University of Illinois Urbana-Champaign, Urbana, IL

Don W. Burgess

Cooperative Institute for Mesoscale Meteorological Studies, University of Oklahoma, Norman, OK

and R. B. Wilhelmson

National Center for Supercomputing Applications, Urbana, IL

1. INTRODUCTION

On May 8, 2003 a tornadic supercell passed through portions of the Oklahoma City metro producing up to F4 damage along its path. This violent storm tracked through the dense, static radar network in central Oklahoma affording a unique data set of multi-platform radar observations for subsequent analysis of this significant event. Here a continuation of the work begun by Burgess (2004) is presented. Numerous studies have documented the structure and evolution of tornadic supercell thunderstorms (e.g., Doswell and Burgess, 1993), largely rooted in analysis via conventional single and dual-Doppler radar observations. Yet, despite an increasing prevalence of polarimetric radar observations, to date no studies have documented the structure and morphology of polarimetric signatures associated with tornadic storms as they relate to the archetypical supercell template. A distinct temporal morphology will be demonstrated for the polarimetric field variables during the May 8, 2003 event, providing indication that strong interrelations may exist between kinematic fields and polarization variables. This work will hopefully inspire similar studies of other supercell events, both tornadic and non-tornadic, to determine the commonality of the observations described herein.

A limited number of studies have sought to characterize polarimetric signatures to severe storm behavior. Illingworth et al. (1987) first identified positive differential reflectivity (hereafter ZDR) columns within isolated developing convective cells. Conway and Zrnić (1993) and later Brandes et al. (1995), with the benefit of in situ aircraft observations, refined the understanding of the ZDR column feature as a deep structure, often extending well above the freezing level, of positive ZDR offset and slightly downshear from the updraft maxima,

presumably where collision / coalescence process within the updraft has allowed a sparse population of drops to grow to quite large (up to 5 mm and increasingly oblate shape) sizes. Hubbert et al. (1998) further detailed a specific differential phase (hereafter KDP) column adjacent to the aforementioned ZDR column and credited this feature to liquid drop shedding (preferentially in the 1-2 mm drop size range) from wet hailstone growth leading to high liquid water content regions. Further, Wakimoto and Bringi (1988) identified a field of significant positive ZDR below the melting level, with a “ZDR hole” feature associated with a wet microburst event which they tied to a local minimum in the apparent height of the melting level – with the microburst developing below this depression in the ZDR height field. The depression in the height of large positive ZDR values above the microburst was presumably within a precipitation shaft dominated by isotropic scattering from tumbling hailstones. Loney et al. (2002) then described in situ observations near the updraft at mid-levels of a supercell thunderstorm and compared calculated polarimetric fields using aircraft sampled particle distributions with polarimetric radar observations. Notably, they were also able to relate the KDP column to melting and shedding of drops along the western flank of the updraft, and linked a ZDR maxima along the eastern flank of the updraft to sparse larger drops dominating the scattering. Finally, Ryzhkov et al. (2005) illustrated polarimetric signatures of non-hydrometeors (tornado debris) which are largely anisotropic scatterers yielding identifiable characteristics that suggest the presence of a tornado vortex owing to the detectable debris.

2. DATA AND METHODOLOGY

The polarimetric radar observations described in this study were collected by KOUN, which is a prototype system for the planned polarization upgrade of the fleet of operational WSR-88D radars (Doviak et al., 2000). KOUN collected continuous data (VCP-11) during the initiation and subsequent maturation including the early tornadic phase of the cell. Subsequently, the radar suffered a power outage

Corresponding author address: Glen S. Romine, Department of Atmospheric Sciences, University of Illinois Urbana-Champaign, 105 S. Gregory St., Urbana, IL, 61801; romine@atmos.uiuc.edu

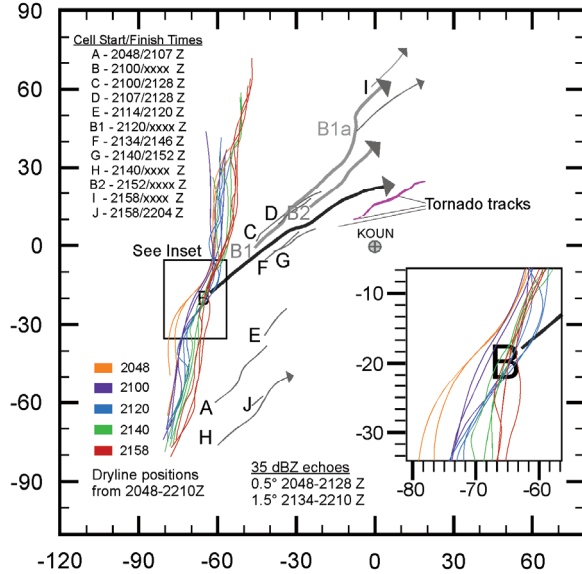


Figure 1: Cell tracks and approximate dryline positions from 2046 – 2210 Z on May 8, 2003 for the ‘focus region’ which was a 200 km^2 domain offset 10 km south and 20 km west of the KOUN radar site (which is at the origin) near Norman, OK. Cell centroids were tracked if two consecutive volume scans showed a distinct echo with $\geq 35 \text{ dBZ}$ using the 0.5° (1.5°) tilt scans from 2048–2128 (2134–2210) Z. Dryline axis locations approximated from ‘clear air’ returns on base scans, color coded by time window (time labels are first time in color grouping).

stemming from damage associated with one of the storm’s tornadoes. As such, polarimetric radar observations available for this study are constricted to the period of continuous collection from approximately 2048–2210 Z on May 8, 2003. The precursor cells developed within 70 km of the KOUN radar and passed within 20 km near the end of the observing period. While several convective features developed during the observing period within range of the KOUN radar, the discussion here is primarily focused on the cell which resulted in the significant tornado event in the Oklahoma City metro region – labeled cell ‘B’ in Fig. 1.

For the benefit of volumetric analysis, radar data collected from KOUN for this event were manually pre-processed to remove ground clutter as well as unfolding of radial velocities (Dowell et al., 2004), which was extended to include subjective cleaning of polarimetric fields of non-meteorological returns using the SOLO II editing tool. Data volumes at a central volume collection time were then created from the sweeps using echo translation and interpolation with a Cressman scheme using a 500 m radius onto a 1 km (500 m) horizontal (vertical) uniform grid.

3. ENVIRONMENT AND OBSERVATIONS

A synoptically evident (Doswell et al., 1993) severe weather pattern was in place the morning of May 8, 2003. Fig. 2 gives the composite chart (Miller, 1972) for the southern plains region that morning with a lee cyclone and attendant dryline poised to surge eastward as an upper level shortwave trough approached the southern plains in west-southwesterly mean mid-level flow. With deep, tropical moisture at low-levels contained by a strong capping inversion, the stage was set for a significant outbreak of severe storms. Synoptic scale ascent associated with the approaching shortwave as well as stronger low-level convergence along the dryline and residual outflow boundaries from overnight convection led to widespread convective development across portions of Kansas by late afternoon, with more isolated convective development further south into portions of central Oklahoma just ahead of the advancing dryline. Between 2000–2100Z several clusters of small convective cells developed just east of the dryline across portions of the focus region shown in Fig. 1, including the cell (labeled track ‘B’) which eventually would mature into the tornadic supercell of interest. As described in greater detail in Burgess (2004), the early stages of the storm featured largely multi-cellular behavior with a transition toward a

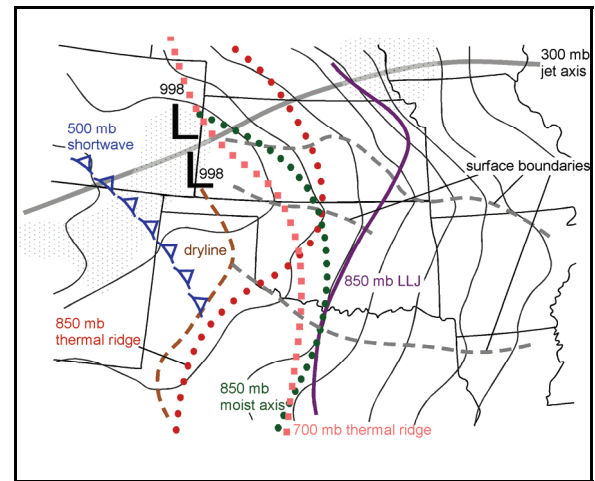


Figure 2: Synoptic environment composite diagram for the Southern Plains for 12 Z on May 8, 2003. Shown are the 300 mb jet axis (heavy gray), 500 mb shortwave axis (blue dashed triangles), 700 mb thermal axis (peach squares), 850 mb thermal and moist axes (red and green circles, respectively), 850 mb low-level jet axis (purple heavy line), surface pressure contours every 2 mb (thin gray), surface dryline (thin dashed brown) and outflow boundaries (thin dashed gray).

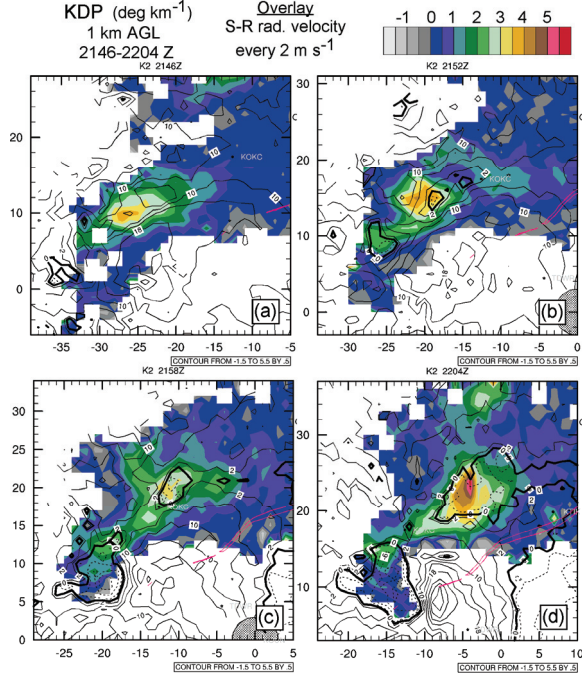


Figure 3: CAPPI at 1 km AGL of KDP (filled contour, every 0.5 deg km⁻¹) overlaid by storm-relative radial velocity (solid [dashed negative] contour, every 2 m s⁻¹ with storm motion of 14 [8] in the E-W [N-S] direction) for the period from 2146-2204 Z every 6 minutes for panels a-d respectively.

more distinct classic supercell by 2140 Z and a fairly rapid cycling thereafter entering the tornadic phase by around 2200 Z.

Early cell evolution demonstrated several of the polarimetric radar observations described in the literature. Similar to Illingworth et al. (1987), cell ‘B’ showed an intermittent elevated positive ZDR column (here defined as a continuous region of 2 dB or greater) extending above 6 km AGL along the upshear echo edge similar to other distinct cells during the early multi-cell phase – though the column feature became consistently more prominent within cell ‘B’ beyond 2120 Z. Additionally, an expanding region of high ZDR below the melting level began near the updrafts of cells, but by 2120 Z began elongating downshear while yielding increasingly higher values, particularly along the right flank of the dominant cell. A KDP column (here defined as a continuous region of 2 deg km⁻¹ or greater) was also established at mid-levels by 2120 Z, contiguous and immediately downshear, centered slightly left of the ZDR column for cell ‘B’ only. Following the hydrometeor identification guidance of Straka et al. (2000), the KDP column aloft was consistent with a mixed phase environment and likely was associated

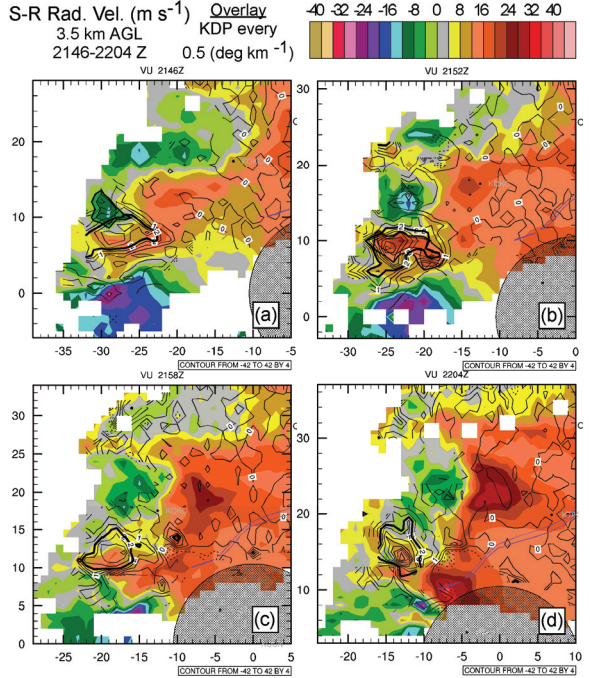


Figure 4: CAPPI at 3.5 km AGL of storm-relative radial velocity (filled contour, every 4 m s⁻¹ with storm motion of 14 [8] in the E-W [N-S] direction) overlaid by KDP (solid [dashed negative] contour, every 0.5 deg km⁻¹) for the period from 2146-2204 Z every 6 minutes for panels a-d respectively.

with wet hail growth aloft, similar to Hubbert et al. (1998). Burgess (2004) identified strengthening mid-level rotation within the storm from 2130-2140 Z, with a rapid increase in both mid-level and particularly low-level rotation beyond 2200 Z.

A particularly intriguing early result from analysis of the polarimetric data included the apparent deformation of the KDP field at low-levels (shown at 1 km AGL) of the storm coincident with the development of a rear flank downdraft surge and subsequent tornadogenesis for this event, as demonstrated in Fig. 3. The deformation of the KDP field, along with strong indications of mid-level entrainment, conspicuously coincided with the detection of a rear flank downdraft surge near the surface. Increasing values of KDP also shifted downshear in a storm-relative sense along with a strengthening convergent boundary in radial winds well within the interior of the storm, along the right edge of the gradient in KDP. Meanwhile, Fig. 4 shows storm-relative velocity contours overlaid with KDP at 3.5 km AGL. From 2146-2204 Z a significant left and rearward directed jetlet in a storm-relative sense is co-located with significant values of KDP just south of a strong anti-cyclonic

vortex (north of the mesocyclone), simultaneous with the broadening concave arc of high KDP below (a.k.a. an expanding surface area of high liquid water content adjacent to drier environmental air) evident in Fig. 3. It is suggested this shell of high liquid water content may have encased the leading edge of a tongue of advancing mid-level environment air just north of the anti-cyclonic vortex along the left flank of the cell as the splitting storms diverged. The combined upshear extension of the KDP column between the counter-rotating vortices along with the expanding concave KDP surface would tend to promote strong evaporational cooling along an expanding surface area in the presence of adequate mixing. Shortly after the beginning of this dry intrusion event, a strong boundary surge (shown in radial convergence) developed, first detected along the left rear flank of the cell immediately adjacent to the left side rearward extension of the KDP maxima at 1 km. The distinct downdraft pulse rapidly swept to the right rear flank, overrunning the former lead edge of the rear flank downdraft gust front while the mid-level mesocyclone shifted from showing a divergent and rotational component in radial winds to almost purely rotation by 2204 Z, as shown in Fig. 4.

Fortunately, the KDP maxima shown in Fig. 3 passed nearly over the KOKC ASOS station (shown at $\sim X=13$, $Y=18$), affording an opportunity to determine if the low-level KDP passage over the site coincided with significant weather trends at the surface. The KOKC meteogram, presented in Fig. 5, is overlain with a box highlighting the time window coinciding with that presented in Figs. 3 and 4. Noteworthy is the lack of significant cooling, and modest moistening up through about 2158 Z despite heavy rain and large hail (0.75) being reported at the station beginning at 2155 Z. Following was a more significant cooling event after 2200 Z with the station then underneath the rearward KDP extension.

4. FUTURE WORK

Presented were some interesting observations of polarimetric field temporal morphology which at least suggest strong spatial relations to kinematic fields both at low levels and aloft which might feed back into thermodynamics, such as rear flank downdraft forcing. Short term research goals include employing TDWR data to better refine inferred surface boundary / gust front locations and fitting the polarimetric features noted from the May 8 event to complement the classic supercell conceptual model description. The implied role of entrainment along the *left* flank of the cell leading to a significant downdraft pulse would seem contrary to traditional thoughts of the rear flank downdraft mid-level air

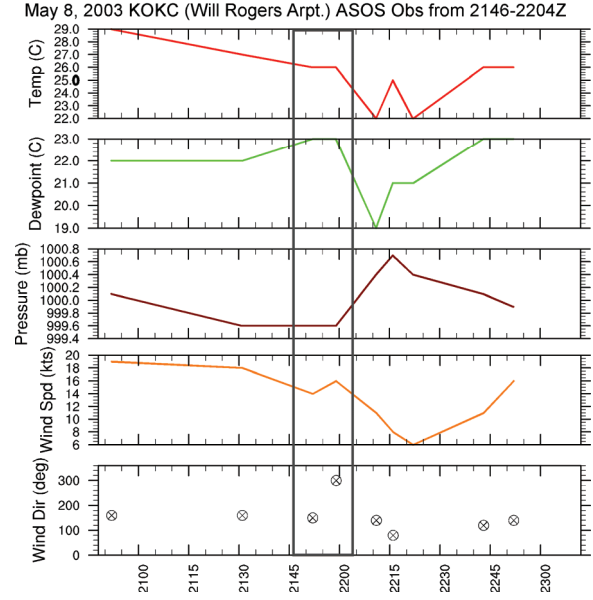


Figure 5: Surface weather observations from the KOKC ASOS station from 2052-2252 Z on May 8, 2003. Shown from top to bottom are traces of temperature ($^{\circ}$ C), dewpoint ($^{\circ}$ C), pressure (mb), wind speed (kts) and direction ($^{\circ}$). Heavy box overlay highlights the time window shown in Figs. 3 and 4.

entrainment originating along the *right* flank of the storm (e.g., Browning, 1964). Given the importance of understanding possible sources of rear flank downdraft forcing and the thermodynamic history of downdraft air, long term project goals include the assimilation of the polarimetric radar fields into a storm-scale EnKF data assimilation system which will provide best guess analyses of the observed storm state enabling a deeper investigation of the relationships between the polarimetric signatures and storm kinematics and may lead to a better understanding of rear flank downdraft mechanisms and thermodynamics.

5. ACKNOWLEDGEMENTS

Portions of this material are based upon work supported by the National Science Foundation under Award No. ATM-0449753. David Dowell graciously provided cleaned reflectivity and unfolded velocity data from the KOUN radar used in this study, as well as providing the objective analysis software utilized throughout this study. Kevin Scharfenberg also provided additional KOUN data and Valery Melnikov supplied radar calibration information. Some plots were generated using NCAR Command Language software.

6. REFERENCES

- Brandes, E.A., J. Vivekanandan, J. D. Tuttle and C. J. Kessinger, 1995: A study of thunderstorm microphysics with multiparameter radar and aircraft observations. *Mon. Wea. Rev.*, **123**, 3129–3143.
- Browning, K. A., 1964: Airflow and precipitation trajectories within severe local storms which travel to the right of the winds. *Mon. Wea. Rev.*, **21**, 634-639.
- Burgess, D. W., 2004: High resolution analyses of the 8 May 2003 Oklahoma City storm. Part I: Storm structure and evolution from radar data. *Preprints, 22nd Conf. Severe Local Storms*, Hyannis, MA, AMS, (CD-ROM).
- Conway, J. W. and D. S. Zrnić, 1993: A study of embryo production and hail growth using dual-Doppler and multiparameter radars. *Mon. Wea. Rev.*, **121**, 2511–2528.
- Doswell, C. A., III, and D. W. Burgess, 1993: Tornadoes and tornadic storms: A review of conceptual models. Chapter of *The Tornado: Its Structure, Dynamics, Prediction, and Hazards*, C. Church, D. Burgess, B. Davies-Jones, C. Doswell (Ed.), American Geophysical Union, Geophysical Monograph #79, Washington DC.
- Doswell, C. A., III, S. J. Weiss and R. H. Johns, 1993: Tornadoes forecasting: A review. Chapter of *The Tornado: Its Structure, Dynamics, Prediction, and Hazards*, C. Church, D. Burgess, B. Davies-Jones, C. Doswell (Ed.), American Geophysical Union, Geophysical Monograph #79, Washington DC.
- Hubbert, J., V. N. Bringi and L. D. Carey, 1998: CSU-CHILL polarimetric measurements from a severe hailstorm in eastern Colorado. *J. Appl. Meteor.*, **37**, 749–775.
- Doviak, R. J., V. Bringi, A. Ryzhkov, A. Zahrai, and D. Zrnic, 2000: Considerations for polarimetric upgrades to operational WSR-88D radars. *J. Atmos. Oceanic Tech.*, **17**, 257-278.
- Illingworth, A. J., J. W. F. Goddard, S. M. Cherry, 1987: Polarization radar studies of precipitation development in convective storms. *Q. J. R. Meteorol. Soc.*, **113**, 469-489.
- Loney, M. L., D. S. Zrnić, J. M. Straka, A. V. Ryzhkov. 2002: Enhanced polarimetric radar signatures above the melting level in a supercell storm. *J. Appl. Meteor.*, **41**, 1179–1194.
- Miller, R.C., 1972: Notes on the Analysis and Severe-Storm Forecasting Procedures of the Air Force Global Weather Central. Air Weather Service Tech. Rept. 200 (Rev.), Air Weather Service, Scott Air Force Base, IL, 190 pp.
- Ryzhkov, A. V., T. J. Schuur, D. W. Burgess and D. S. Zrnić. 2005: Polarimetric Tornado Detection. *J. Appl. Meteor.*, **44**, 557–570.
- Straka, J. M., D. S. Zrnić, A. V. Ryzhkov, 2000: Bulk hydrometeor classification and quantification using polarimetric radar data: Synthesis of relations. *J. Appl. Meteor.*, **39**, 1341–1372.
- Wakimoto, R. M., and V. N. Bringi, 1988: Dual-polarization observations of microbursts associated with intense convection: The 20 July storm during the MIST Project. *Mon. Wea. Rev.*, **116**, 1521–1539.